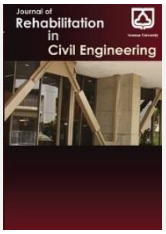

Journal of Rehabilitation in Civil Engineering

Journal homepage: https://civiljournal.semnan.ac.ir/

Experimental Investigation of Hybrid FRP Bonding for Strengthening Steel Plates and Beam Sections under Static Loading

Darshan Parakhiya[1]; Husain Rangwala [1 *]; Amit Thoriya [1]; Tarak Vora [1]

1 Department of Civil Engineering, Marwadi University, Rajkot, India
* Corresponding author: *husain.rangwala@marwadieducation.edu.in*

ARTICLE INFO

Article history:
Received: 30 May 2025
Revised: 30 July 2025
Accepted: 17 August 2025

Keywords:
Adhesive bonding;
Strengthening;
FRP;
Hybrid retrofitting;
Tensile testing.

ABSTRACT

This study presents an experimental investigation into the tensile and flexural performance of steel members strengthened using Fiber Reinforced Polymer (FRP) composites, specifically Carbon FRP (CFRP) and Glass FRP (GFRP). Mild steel plates (600 mm × 50 mm × 6 mm) were tested under axial tension, with FRP sheets applied in single-layer (SL) and double-layer (DL) configurations. Strengthening was further enhanced using mechanical anchorage techniques such as grooving and end-plate bolting. For flexural testing, two steel section types, Channel Section (CS) and Rectangular Hollow Section (HS), each 1000 mm in length, were retrofitted with externally bonded CFRP and GFRP sheets and subjected to four-point bending. Key parameters studied include ultimate load, yield strength, initial stiffness, ductility, and energy absorption. The results demonstrate that DL configurations significantly improve both strength and stiffness compared to SL counterparts, while anchorage mechanisms effectively delay debonding and enhance overall structural performance. Among the FRP types, CFRP exhibited higher load capacity, whereas GFRP showed relatively higher ductility in some cases due to better bond distribution. While the findings confirm the effectiveness of FRP strengthening in enhancing structural behavior, the study is still limited by the use of small-scale specimens and simplified boundary conditions, which may affect full-scale generalization. Future work could address long-term durability and field-level performance under varying load conditions.

E-ISSN: 2345-4423

How to cite this article:
Parakhiya, D., Rangwala, H., Thoriya, A. and Vora, T. (2026). Experimental Investigation of Hybrid FRP Bonding for Strengthening Steel Plates and Beam Sections under Static Loading. Journal of Rehabilitation in Civil Engineering, 14(2), 2359. https://doi.org/10.22075/jrce.2025.2359

1. Introduction

Steel structures are extensively employed in civil infrastructure due to their superior strength, ductility, and durability. However, retrofitting steel members using externally bonded Fiber Reinforced Polymer (FRP) laminates presents significant challenges compared to concrete substrates. The smooth, non-porous surface of steel, along with its susceptibility to corrosion, often leads to poor adhesive interaction and premature debonding failures [1,2]. FRP composites, particularly Carbon FRP (CFRP) and Glass FRP (GFRP), have shown great potential for enhancing the load-bearing and flexural performance of steel elements due to their high strength-to-weight ratio, corrosion resistance, and ease of application. Despite these advantages, the bond performance between FRP and steel is highly sensitive to surface conditions and loading environments. Adhesive bonding alone may not be sufficient, especially under tensile or cyclic loading, if proper surface preparation is lacking [3].

While considerable research has focused on adhesive bonding, the combined effect of surface modification techniques (e.g., grooving) and mechanical anchorage (e.g., bolted end connections) remains underexplored in the context of steel retrofitting. Addressing this gap is critical for developing hybrid strengthening strategies that improve both load capacity and long-term durability.

2. Literature review

Bonding between FRP and steel is affected by several interdependent factors: adhesive selection, surface preparation, joint geometry, and environmental exposure. Proper surface preparation, including sandblasting and solvent cleaning, is critical to enhancing mechanical interlock and removing contaminants that weaken adhesion [1,4]. Poor surface quality leads to rapid degradation of bond strength under moisture and cyclic loading [5]. Toughened adhesives, particularly rubber-toughened epoxies, have demonstrated improved fracture energy and ductility across the bond line, reducing the risk of brittle interfacial failure [3,6]. However, bond thickness must be carefully controlled; while increased thickness can improve energy absorption, it may also reduce stiffness and overall efficiency [7]. Environmental durability is another key consideration. Elevated temperatures near the adhesive's glass transition point, as well as prolonged humidity exposure, can lead to bond degradation [5,8]. Bond performance reductions at high temperatures stress the importance of selecting thermally stable adhesives for critical applications [9]. and Silva et al. observed bond degradation under freeze–thaw cycles, underscoring the vulnerability of adhesive interfaces to climatic variations [10]. Geometric factors such as bond length and joint configuration (e.g., single vs. double shear) influence stress distribution. The optimized bond lengths improve load transfer until an effective threshold, beyond which additional length has minimal effect [7,11]. Hybrid bonding systems that incorporate mechanical fastening have gained prominence. The bolted connections in FRP-steel joints enhance ultimate load capacity and delay debonding [12]. A steel plate hybrid bonding method was developed to reinforce adhesive bonds under flexural loading [2]. Recent innovations such as nanofiber veils embedded in adhesive layers show promise in improving bond toughness and controlling crack propagation. The veils increase interface ductility and delay debonding under dynamic loading conditions [11]. Previous investigations by the researchers studied the FRP bolts and hybrid bonding systems in FRP steel interfaces, which show preliminary insights into adhesive performance and mechanical anchorage, but did not fully evaluate multi-layered systems or flexural behavior [12,13].

Beyond bonding mechanics, extensive experimental evidence supports the effectiveness of CFRP in enhancing the structural performance of various steel members. Sivasankar et al. reported a 30% increase in axial capacity for wrapped Square Hollow Steel columns [14], while Rangwala et al. showed recovery

of lost strength in steel members under combined stresses [15,16]. Jagtap and Pore observed up to 30% load improvement in CFRP-strengthened I-beams [17], and Weerasinghe et al. confirmed enhanced flexural performance in curved hollow sections with optimized bond lengths[18]. Regmi and Azadeh reported flexural gains of up to three times in damaged beams[19]. Li et al. noted bond enhancement from surface corrosion but a reduction under wet–dry cycles [20]. Li et al. highlighted that ductile adhesives improve shear capacity[21], Tafsirojjaman et al. demonstrated improved energy dissipation and moment capacity in GFRP/CFRP-strengthened under cyclic loads [22,23], while Hu et al. confirmed CFRP's ability to delay fatigue-induced crack growth [24]. Regmi and Azadeh also proposed fatigue life models for basalt/aramid FRP-retrofitted beams. Liu et al. introduced a CFRP–steel tube system with enhanced ductility [25], and Tahmasebinia et al. validated CFRP's impact resistance via simulation [26]. Anchorage methods remain crucial for bond reliability, and environmental sensitivity continues to influence long-term performance [27]. Alam et al. further highlighted CFRP's role in energy absorption under impact, proposing PMO_3 as a promising binder [28].

Recent studies have enhanced the understanding of FRP steel systems through advanced modeling and experimental validation [29,30]. Techniques such as machine learning are applied to calibrate bond strength in textile-reinforced masonry [31]. The creep behavior of CFRP–steel joints was analyzed experimentally and numerically [32,33]. Soft computing methods are utilized to estimate shear and flexural capacities in FRP-reinforced concrete [34,35].

Despite the growing application of Fiber Reinforced Polymer (FRP) systems for retrofitting steel structures, limited research has systematically compared the performance of different strengthening configurations like (i) adhesive-bonded CFRP and GFRP laminates in single-layer (SL) and double-layer (DL) forms, (ii) laminates bonded to transversely grooved steel surfaces for improved mechanical interlock, and (iii) hybrid bonding combining adhesive with bolted anchorage to delay debonding and enhance load transfer under both tensile and flexural loading. Moreover, there is a lack of integrated studies that explore the effect of section geometry and mechanical anchorage techniques on the structural efficiency of FRP retrofits. This study aims to fill this knowledge gap by conducting a detailed experimental investigation into the tensile and flexural behavior of steel members strengthened with CFRP and GFRP sheets. The primary objectives are to evaluate the influence of FRP type and layer configuration on strength, stiffness, and ductility, assess the effect of hybrid bonding methods, and compare performance differences between tensile and flexural retrofitting for various cross-sectional geometries. The findings aim to provide practical insights for optimizing retrofit strategies for steel structures subjected to different loading conditions.

3. Experimental program

This study follows a structured experimental approach to evaluate the tensile and flexural performance of FRP-strengthened steel elements. The methodology includes material selection, preparation of specimens across multiple retrofit configurations, and mechanical testing using standardized procedures. The following subsections detail the materials, preparation techniques, and experimental setups used.

The experimental program was designed to evaluate the strengthening performance of FRP composites applied to steel structural elements under tensile and flexural loading. The study focused on two primary components: (1) strengthening of mild steel plates under axial tension and (2) strengthening of steel beams under flexural loads. The overall flow of the study is shown in Fig. 1.

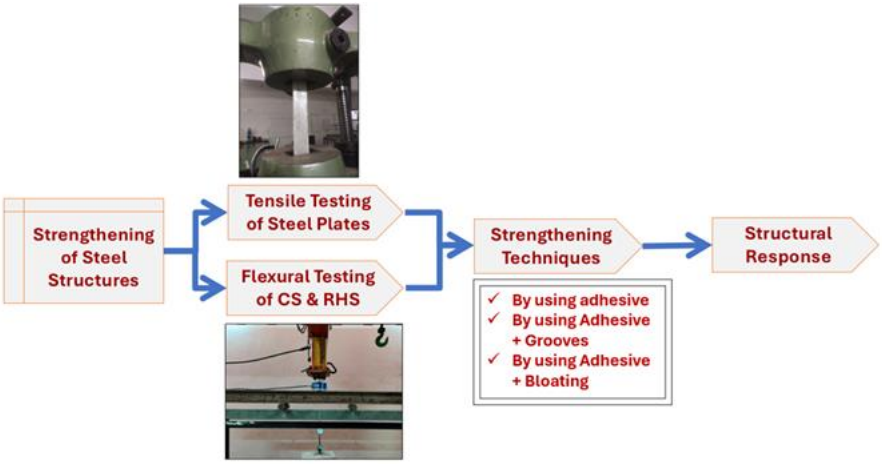

Fig. 1. Flowchart for overall process of the experimental study.

3.1. Material properties

The base material consisted of carbon steel plates conforming to IS or ASTM standards. These specimens exhibited yield strengths in the range of 250–500 MPa, ultimate tensile strengths between 400–600 MPa, and an elastic modulus of approximately 200 GPa. CFRP sheets used in the study were unidirectional laminates (e.g., SikaDur, MBrace) with a thickness ranging from 0.17 to 1.4 mm, tensile strengths up to 5000 MPa, and modulus of elasticity between 200 to 250 GPa. The typical Poisson's ratio was approximately 0.3 [36,37]. Sheets were aligned longitudinally for the direction of load application to optimize mechanical performance. The mechanical and geometric properties of the test specimens are as shown in Table 1.

Table 1. Mechanical and Geometric Properties of Test Specimens.

Specimen	Property	Range
Steel Plate	Yield Strength	250–500 MPa
	Ultimate Tensile Strength	400–600 MPa
	Modulus of Elasticity	200 GPa
	Dimension	600 mm × 50 mm × 6 mm
CFRP Sheet	Type	Unidirectional laminate (Sikadur / MBrace)
	Thickness	1.2 mm
	Tensile Strength	Up to 5000 MPa
	Modulus of Elasticity	200 GPa
	Poisson's Ratio	0.3
GFRP Sheet	Thickness	1.2 mm
	Tensile Strength	Up to 1000 MPa
	Modulus of Elasticity	70 GPa
Channel Section Beam	Cross-Section	75 × 40 × 5 mm
	Span	1000 mm
Rectangular Hollow Beam Section	Cross-Section	60 × 40 × 4 mm
	Span	1000 mm

3.2. Specimen preparation

All tensile test specimens were prepared using mild steel plates measuring 600 mm × 50 mm × 6 mm, each featuring a centrally located 17 mm diameter circular hole. The specimen dimensions and configurations for tensile and flexural testing were selected based on common practice in previous FRP-

steel retrofit studies. A hole was introduced at the center of each steel plate to simulate the stress concentration effect common in bolted connections and to assess the contribution of FRP in strengthening against net-section fracture, as shown in Fig. 3 (b) and (c). The ratio of net area to gross area (A_n/A_g) for the cross-section was calculated to be approximately 0.66, providing a basis for analytical comparison with FRP-strengthened specimens [38]. The specimens were classified into three major strengthening categories based on the bonding technique employed:

Category I: Steel plates strengthened with adhesively bonded CFRP/GFRP laminates in both single-layer (SL) and double-layer (DL) configurations.

Category II: Steel plates retrofitted with adhesive bonding combined with transversely machined grooves (at 50 mm intervals) to improve mechanical interlocking, again using CFRP/GFRP in SL and DL formats.

Category III: Steel plates strengthened through a hybrid method that integrated adhesive bonding with bolted end connections to provide additional mechanical anchorage.

Each configuration was evaluated against an unstrengthened control specimen (NP) to quantify the improvement in tensile performance. The dimensions and positioning of the FRP laminates were kept consistent across categories, using unidirectional CFRP/GFRP strips cut to 500 mm × 40 mm × 1.2 mm. The FRP laminates were adhesively surface-bonded along the central 500 mm length of the 600 mm long steel plates, leaving 50 mm unbonded at each end for gripping and observation. A solvent-free, two-part epoxy adhesive (Sikadur-30) was selected for bonding. The adhesive demonstrated tensile strengths around 40 MPa and elastic moduli in the range of 2–4 GPa. Before bonding, steel surfaces were prepared through degreasing with acetone and surface treatment using sandblasting or grit-blasting to achieve surface roughness levels of 20–50 μm, thereby improving adhesive interfacial strength. After the application of CFRP and GFRP laminates using a two-part structural epoxy adhesive, all specimens were cured under controlled ambient laboratory conditions. The curing environment was maintained at a temperature of 27 ± 2 °C and a relative humidity of 60 ± 5%. Specimens were kept undisturbed on flat steel plates to avoid premature debonding or misalignment. No external heat source or accelerated curing method was used in this study. The regular plate (NP) is shown in Fif. 2 (a). The various specimen configurations and strengthening layouts are clearly illustrated in Fig. 2 (b), Fig. 2 (c), and Fig. 2 (d), while the experimental test setup for tensile testing is presented in Fig. 3.

(a)

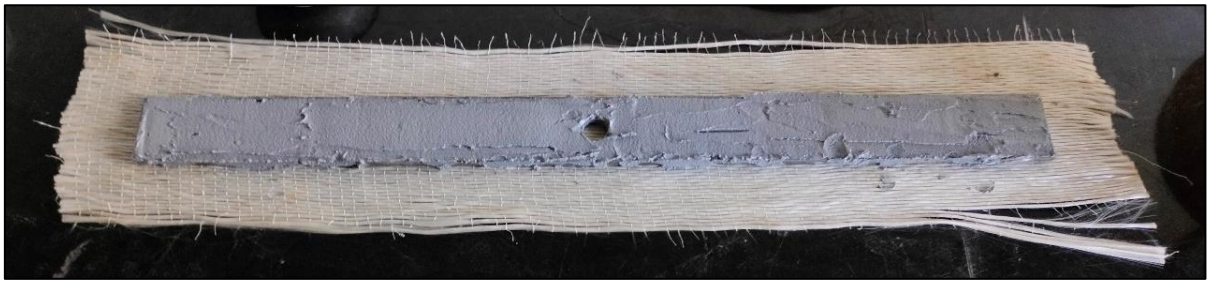

(b)

(c)

(d)

Fig. 2. (a) Regular Steel Plate (NP) (b) Steel Plate with Surface Bonded FRP (c) Steel Plate with Grooves (d) Steel Plates with Bolted Connections.

Fig. 3. Experimental Setup: (a) Tensile Testing of Plates, (b)Flexural Testing of Channel Section.

The Hart-Smith model provides an analytical solution for bonded joints, particularly double-lap joints, where the adhesive shear stress distribution and effective bond length can be estimated from the following equation, where L_{eff} is the effective bond length, E_{FRP} is the modulus of elasticity of CFRP, t_{FRP} is the thickness of FRP, t_{adh} is the thickness of epoxy adhesive, and τ_{max} is the maximum adhesive shear stress [39].

$$L_{eff} = \sqrt{\frac{E_{FRP} \times t_{FRP} \times t_{adh}}{2 \times \tau_{max}}} \quad (1)$$

The calculation gives the bond length of 58.7 mm, which is sufficient for complete stress transfer under ideal bonding conditions. Tensile testing of plates was conducted using a calibrated Universal Testing

Machine (UTM) under displacement control. Specimens were clamped vertically, and a tensile force was applied until failure occurred.

Flexural testing of steel beams was performed using a custom loading frame in a four-point bending configuration. A hydraulic jack applied the load centrally, while deflections at mid-span were recorded using a dial gauge for precise displacement measurement. This setup, shown in Fig. 3, ensured stable load application and accurate capture of flexural behaviour.

4. Results and discussion

This section presents the experimental findings and analysis of tensile and flexural tests conducted on FRP-strengthened steel specimens. The performance of various retrofitting strategies, including different FRP types, layer configurations, and anchorage methods, is evaluated in terms of load-bearing capacity, ductility, failure modes, and overall structural behaviour. The results are discussed comparatively to identify the most effective strengthening techniques.

4.1. Tensile testing of FRP-strengthened steel plates

Tensile tests were conducted on mild steel plates retrofitted with CFRP and GFRP laminates to evaluate their performance under axial tension. The objective was to assess the influence of laminate type (CFRP vs. GFRP), number of layers (single vs. double), and bonding strategies on the tensile strength and ductility of the strengthened specimens. The test matrix also included regular plates as control specimens for benchmarking purposes.

4.1.1. Strengthening of mild steel plates bonded with adhesives

Fig. 4 shows the tensile performance of steel plates strengthened with unidirectional GFRP and CFRP laminates bonded using epoxy in single-layer (SL) and double-layer (DL) configurations. The control specimen (NP) exhibited a peak load of 120.38 kN with a 16.25 mm displacement, displaying elastic–plastic behaviour followed by abrupt failure.

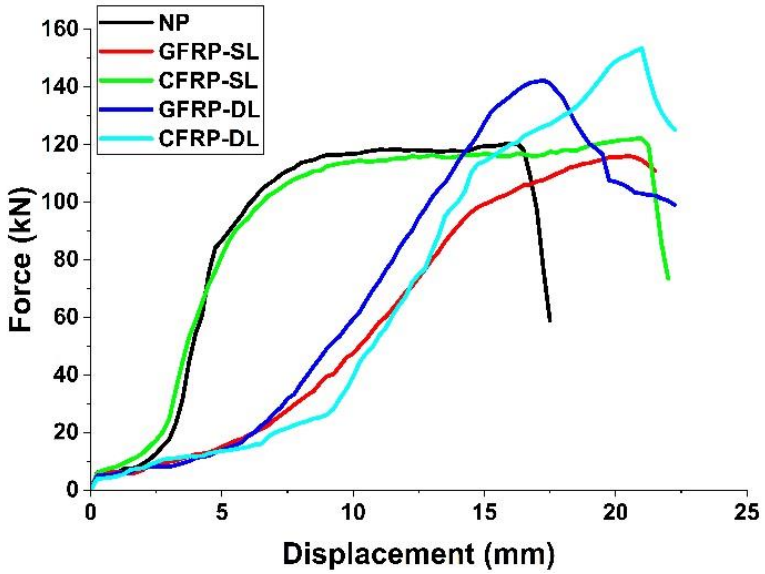

Fig. 4. Force-Displacement of Normal Plates and Plates Surface Applied with GFRP and CFRP using Single-layer and Double-layer.

The GFRP-SL specimen demonstrated a slightly reduced strength of 116.02 kN. In GFRP-SL specimens, visual debonding was observed before reaching the ultimate load. The initial debonding was noticed at approximately 85 kN and 14.2 mm displacement. The steel had already entered yielding, indicating that

debonding was a post-yield but pre-peak failure mechanism. The ductility index is calculated by taking the ratio of the maximum displacement to the yield displacement. From the results, it is calculated that the ductility index for the control specimen (NP) is 1.55 (16.25/10.5) while for the GFRP-DL it is 2.11 (17.5/8.3) as shown in Table 2. The increase in ductility suggests that while bonding limitations impaired full load transfer, the inherent flexibility of GFRP allowed greater energy absorption. Despite exhibiting higher ultimate strengths, double-layered CFRP and GFRP specimens showed slightly lower ductility indices compared to their single-layer counterparts. This reduction in ductility is attributed to the increased axial stiffness of DL configurations, which restricts deformation and promotes brittle laminate cracking or abrupt interface failure. In contrast, the SL systems exhibited more gradual debonding and stress redistribution, resulting in larger displacement before failure and hence higher ductility. In contrast, the CFRP-SL specimen attained a marginal strength gain (122.50 kN) and 21.50 mm displacement. The high stiffness of CFRP contributed to this improvement, although suboptimal bonding limited full performance.

Table 2. Ductility Comparison for Mild Steel Plates Bonded with Adhesives.

Specimen	Yield Disp. (mm)	Failure Disp. (mm)	Ductility Index
NP (Control)	10.5	16.25	1.55
GFRP-SL	8.5	20.5	2.41
CFRP-SL	9.2	21.5	2.34
GFRP-DL	8.3	17.5	2.11
CFRP-DL	10.0	22.5	2.25

The significantly higher initial stiffness observed in CFRP specimens, as shown in Fig. 4. This is primarily due to the increased axial rigidity resulting from the additional CFRP layer. The improved bond interface and greater confinement reduce early deformation, leading to a steeper initial slope in the force-displacement response.

The application of double layers (DL) led to significant enhancements. GFRP-DL reached 142.30 kN, a 22.6% increase over GFRP-SL and 18.2% over NP. The failure displacement was 17.50 mm, reflecting improved load transfer and moderate ductility. The CFRP-DL configuration achieved the highest tensile strength, recording 153.30 kN, 27.3% above NP and 25.6% over CFRP-SL, with a failure displacement of 22.50 mm, indicating a well-balanced performance in terms of strength, stiffness, and ductility.

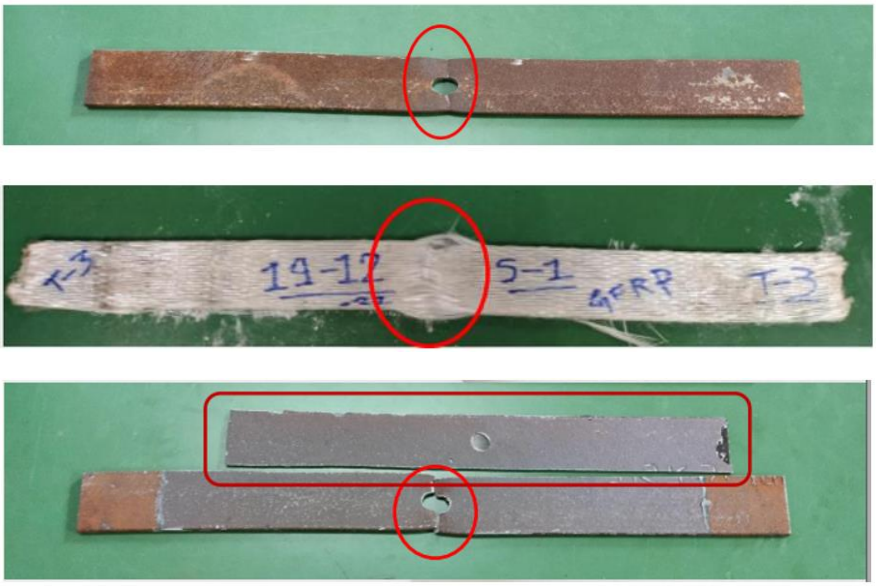

Fig. 5. Failure Pattern of (a) Regular Steel Plate (NP), (b) Steel Plate Surface Applied with GFRP with double layer (GFRP-DL), and (c) Steel Plate Surface Applied with CFRP using Single layer (CFRP-SL).

Failure patterns as shown in Fig. 5 revealed that GFRP specimens generally failed via gradual fibre rupture and adhesive debonding, while CFRP exhibited localised laminate cracking due to higher stiffness. Premature debonding was more prominent in SL specimens, especially for GFRP.

Double-layered retrofitting significantly improved both strength and ductility, with CFRP-DL demonstrating the highest performance. DL specimens are more likely to fail due to laminate rupture or cohesive cracking at higher loads, which are sudden. SL specimens, on the other hand, fail gradually due to interface debonding, allowing more deformation before full separation. The findings emphasize the critical role of bond quality in achieving optimal FRP–steel interaction. Enhanced bonding techniques are essential for maximizing retrofit effectiveness.

4.1.2. Strengthening of mild steel plates bonded with adhesives using grooves

To enhance the bond integrity between FRP laminates and steel, transverse grooves were introduced on the steel plate surface at 50 mm intervals. These grooves acted as mechanical interlocks, improving shear resistance and adhesive penetration. The resulting load-displacement responses and failure patterns for single-layer (SL) and double-layer (DL) GFRP and CFRP retrofitted specimens are illustrated in Fig. 6, with corresponding failure modes shown in Fig. 7.

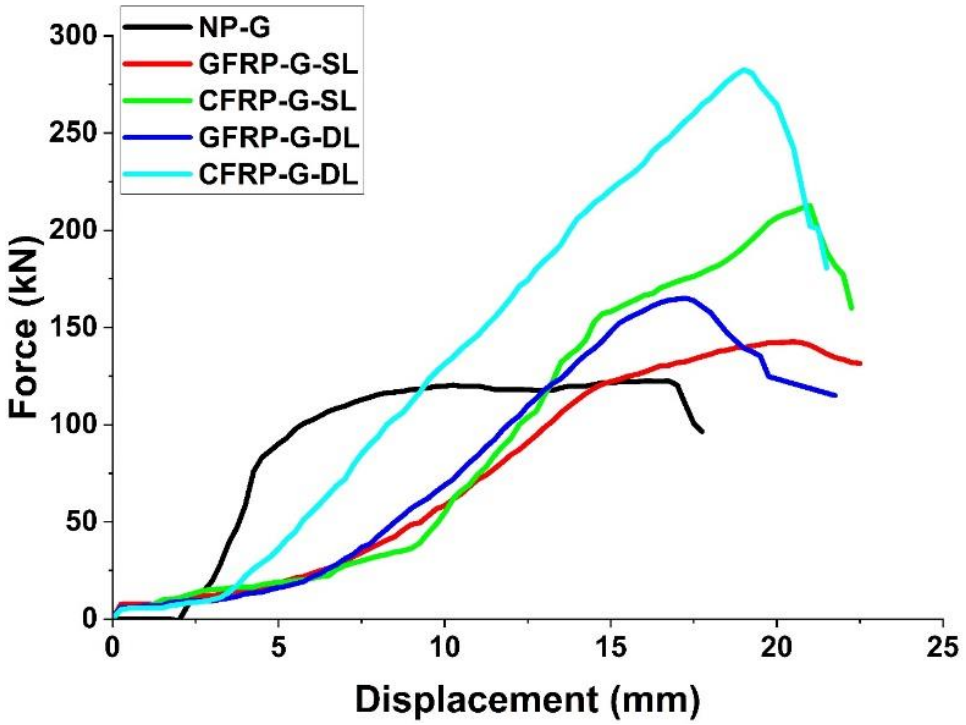

Fig. 6. Force-Displacement of Normal Plates and Plates with Grooves Surface Applied with GFRP and CFRP using Single-layer and Double-layer.

The control grooved specimen (NP-G) achieved a baseline peak load of 122.50 kN with a displacement of 16.75 mm. Retrofitting with GFRP-SL over grooved surfaces increased the peak load by 16.5%, while failure displacement also improved, indicating enhanced energy dissipation. Failure observations revealed delayed debonding and gradual fiber rupture, validating the improved interfacial behavior due to mechanical confinement.

The CFRP-SL-Grooved specimen showed a peak load increase of approximately 34.75% over NP-G (122.5 kN), reaching 165 kN. The load-displacement curve in Figure 8 indicates a reduced post-yield slope and early stiffness loss, consistent with local debonding followed by laminate cracking. The ductility, although lower than GFRP's, reflects CFRP’s higher stiffness and more brittle failure behavior.

The GFRP-DL-Grooved specimen achieved a 73.60% increase in peak load over NP (122.5 kN) and approximately 49% over GFRP-SL-Grooved. However, the failure displacement was slightly lower than that of the SL-Grooved specimen, indicating higher stiffness but slightly reduced ductility. This suggests that while double layers enhance strength, they also increase the stiffness of the bonded zone, which can limit deformation capacity.

The GFRP grooved specimens failed due to Gradual fiber rupture and groove shear slip, while the CFRP specimens failed due to Laminate cracking and cohesive epoxy failure, as shown in Fig. 7. Both GFRP and CFRP grooved specimens exhibited controlled, cohesive failure with significantly reduced debonding. The mechanical confinement provided by grooves effectively resisted adhesive peel and shear, preserving the integrity of the FRP–steel interface. It was observed that grooved specimens predominantly failed due to cohesive debonding and fiber rupture near the groove location.

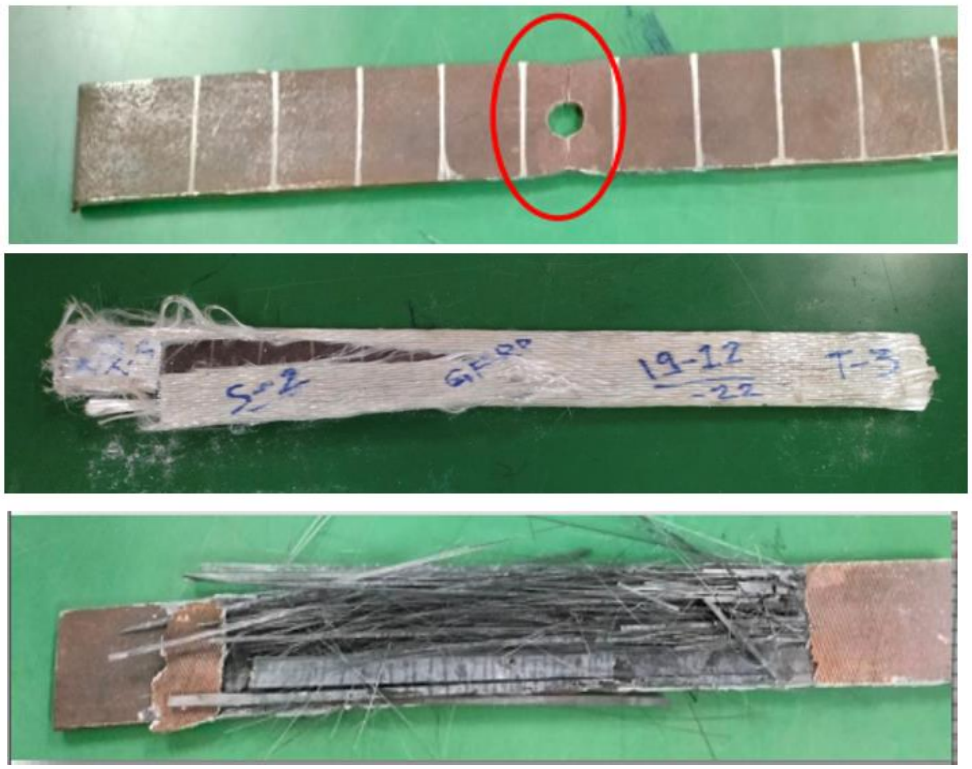

Fig. 7. Failure Modes for Grooved Steel Plates: (a) NP-G local yielding and tearing at hole edge, (b) GFRP-DL-Grooved gradual fiber rupture and adhesive shear-out, and (c) CFRP-DL-Grooved localized laminate cracking and partial delamination near groove location.

Grooving notably improves the bonding and mechanical performance of FRP-strengthened steel plates. CFRP-DL-Grooved is optimal for strength-focused applications, while GFRP-DL-Grooved excels in ductility and energy absorption. Single-layer systems offer economical options with moderate enhancement.

4.1.3. Strengthening of mild steel plates bonded with adhesives and bolted connections

To further improve bond reliability and prevent premature debonding, a hybrid retrofitting approach was employed, combining epoxy adhesive bonding with mechanical anchorage using end bolts. This method was tested under tensile loading for GFRP and CFRP in both single-layer (SL) and double-layer (DL) configurations. The corresponding load-displacement responses are shown in Fig. 8.

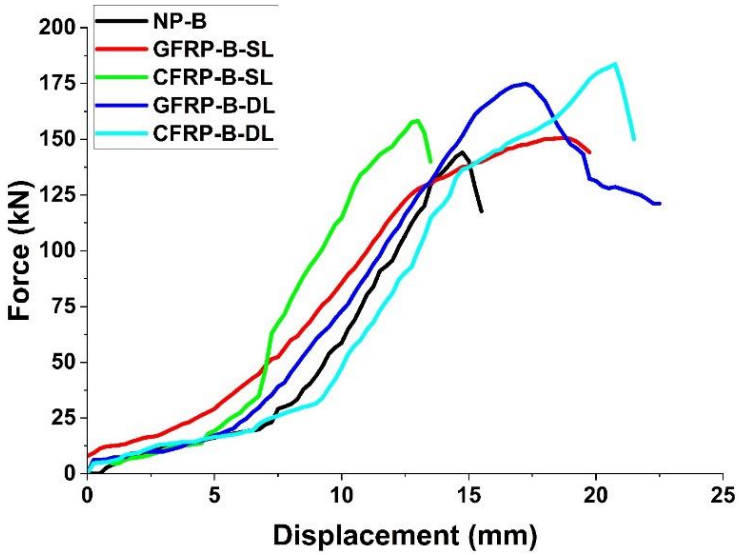

Fig. 8. Force-Displacement of Bolted Plates and Bolted Plates with GFRP and CFRP using Single-layer and Double-layer.

The bolted control specimen (NP-B) exhibited a peak tensile load of 144.00 kN and a failure displacement of 15.45 mm, establishing the reference behavior of bolted steel without FRP reinforcement. Introducing GFRP-B-SL resulted in a modest 4.67% increase in strength, reaching 150.77 kN, while also significantly improving ductility (19.78 mm). This configuration demonstrated favourable energy dissipation and is suited for applications requiring moderate strength and high deformability.

The CFRP-B-SL system further improved load capacity, achieving 158.25 kN (9.85% over NP-B). However, its failure displacement dropped to 13.50 mm, due to CFRP's inherent brittleness and stiffness. Although stronger, this configuration showed early laminate cracking and limited deformation capacity, indicating its preference for static, high-stiffness demand scenarios.

Double-layer retrofitting amplified these benefits. GFRP-B-DL reached 178.87 kN, a 21.40% increase over NP-B, and a 23.75 mm failure displacement, the highest among all specimens, reflecting excellent ductility and strain energy absorption. Progressive fibre rupture and adhesive yielding confirmed effective load-sharing and interface performance. This system is ideal for applications involving cyclic or seismic loads.

The CFRP-B-DL configuration exhibited the highest tensile strength, reaching 183.70 kN, a 27.5% increase over NP-B. Although its ductility (17.50 mm) was less than that of GFRP-B-DL, it still provided a strong balance of strength and deformability. The cohesive failure and laminate cracking verify optimal utilization of both bonding mechanisms.

CFRP-B-DL led in stiffness and capacity, suitable for high-load structural retrofits. GFRP-B-DL, although slightly weaker, exhibited superior deformation behaviour, making it more suitable for energy-absorbing applications. Single-layer variants offered economic alternatives, with GFRP-SL favouring ductility and CFRP-SL favouring stiffness. Bolted hybrid specimens exhibited a combination of CFRP fracture and end-anchor peeling.

Combining bolts with adhesive bonding boosts load capacity and mitigates debonding issues. CFRP-B-DL suits high-strength demands, while GFRP-B-DL is preferable for ductile, energy-absorbing applications. This validates hybrid bonding as a reliable steel retrofitting strategy.

To evaluate the relative effectiveness of strengthening techniques, a comparison was made between CFRP-DL specimens across three configurations: adhesive-bonded (CFRP-DL), grooved (CFRP-DL-G), and hybrid-bonded with bolts (CFRP-B-DL). As shown in Figures 4, 6, and 8, a progressive improvement

in both ultimate load and ductility is observed. The CFRP-DL configuration recorded a peak load of 153.3 kN, which increased to 278.0 kN with grooving and 183.7 kN with hybrid anchorage, as shown in Table 3. Grooving enhanced the mechanical interlock, significantly improving load transfer efficiency, while bolted ends mitigated peel-off and improved post-yield resistance.

Table 3. Comparison of tensile performance of CFRP with adhesive, grooving, & end-plate anchorage.

Configuration	Peak Load (kN)	Failure Displacement (mm)	Ductility
CFRP-DL (adhesive only)	153.3	22.5	2.25
CFRP-DL-Grooved	278.0	21.2	2.12
CFRP-B-DL (bolted)	183.7	17.5	1.75

In addition to maximum load comparisons, the initial stiffness of each specimen was analyzed to identify the elastic response of FRP-strengthened steel members. Stiffness was calculated from the slope of the initial linear portion of the force-displacement curves. Results indicate that double-layer (DL) specimens consistently exhibited higher stiffness than their single-layer (SL) counterparts. For example, the CFRP-B-DL specimen showed an approximate 80–100% increase in initial stiffness compared to CFRP-B-SL, while GFRP-DL specimens demonstrated 60–75% improvement over GFRP-SL configurations. This enhancement is attributed to the increased axial rigidity and improved bond performance with additional composite layers. Stiffness trends were found to align with load capacity increases, although some variations were observed due to anchorage effects and bond condition.

In summary, the experimental investigation demonstrated that double-layered FRP retrofitting substantially enhances both the load-bearing capacity and ductility of steel plates under tensile loading. Among all configurations, CFRP-DL consistently delivered the highest strength, particularly when combined with grooves or mechanical bolts, making it ideal for strength-critical applications. GFRP-DL, while slightly lower in peak load, provided excellent ductility and energy absorption, proving more suitable for structures subjected to cyclic or seismic loads. The introduction of surface grooves significantly improved interfacial bonding and delayed debonding, while hybrid bonding with end bolts further reinforced the connection and load transfer. These findings highlight the critical role of bonding strategy, whether through grooves or mechanical anchorage, in maximizing the structural performance of FRP-strengthened steel elements. Additionally, precision in bolt placement and alignment is critical during retrofitting to ensure uniform load sharing and avoid premature failure. These factors underline the need for careful detailing, quality control during installation, and further research into optimizing hybrid retrofit techniques for field applications.

4.2. Strengthening of steel beams under flexural loading

The flexural testing program was conducted on two types of steel beams: Channel Section (CS) and Rectangular Hollow Section (HS), each with a total length of 1000 mm. The beams were simply supported over a clear span of 800 mm, with loading applied through a four-point bending setup to generate a constant moment region using a servo-controlled hydraulic actuator at a displacement-controlled rate of 2 mm/min until failure. All specimens were fabricated from mild steel conforming to IS 2062, with a nominal yield strength of 250 MPa. The beams were externally strengthened with CFRP or GFRP laminates on the tension face using a high-strength epoxy adhesive. Dial gauges were used to record mid-span deflection at regular load intervals. The support and loading rollers were steel cylindrical pins, allowing horizontal rotation, ensuring near-ideal simply supported boundary conditions. Accordingly, the flexural strengthening phase of this study focused exclusively on CFRP laminates applied under hybrid bonded conditions, targeting the most promising configuration for improving the structural performance of steel channel sections and rectangular hollow sections (HS) under flexural loading. The overall setup of the flexural testing of the beam is shown in Fig. 9.

Fig. 9. Flexural Testing (a) Beam without FRP, (b) Beam with FRP.

4.2.1. Strengthening of steel channel sections

Steel channel sections (CS) were tested in three configurations: unstrengthened (CS), strengthened with single-layer CFRP (CS-CFRP-SL), and with double-layer CFRP (CS-CFRP-DL). CFRP laminates were bonded along the tension face using Sikadur®-300 epoxy.

The load-displacement response is obtained as shown in Fig. 10. The overall results of the flexural test are shown in Table 4.

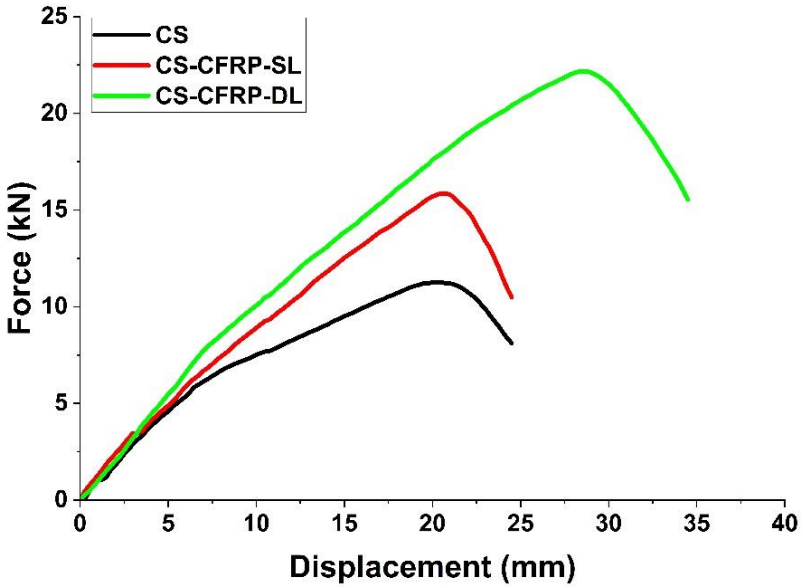

Fig. 10. Force-Displacement of Channel Sections.

The control specimen (CS) failed at a peak load of 11.27 kN with a displacement of 20.75 mm, displaying brittle fracture with negligible post-peak ductility.

The single-layer CFRP-Surface Applied specimen (CS-CFRP-SL) improved the load capacity to 15.85 kN (a 40.6% increase) with comparable displacement, showing enhanced stiffness and better energy dissipation.

The double-layer configuration (CS-CFRP-DL) achieved the highest performance, recording a peak load of 22.17 kN, a 96.6% improvement over the control, and the maximum displacement of 28.50 mm, indicating enhanced ductility and load redistribution capability.

These results confirm that CFRP Surface Applied significantly improves both strength and deformation capacity of steel channels, with double-layer retrofitting proving the most effective for flexural enhancement.

Table 4. Flexural Performance of Channel Sections.

Specimen	Peak Load (kN)	Displacement at Peak Load (mm)	Improvement in Load Capacity Over CS
CS	11.27	20.75	Baseline
CS-CFRP-SL	15.85	20.75	+40.6%
CS-CFRP-DL	22.17	28.50	+96.6%

4.2.2. Strengthening of steel rectangular hollow sections

Mild steel rectangular hollow sections (HS) were similarly evaluated under flexural loading in unstrengthened (HS), single-layer CFRP (HS-CFRP-SL), and double-layer CFRP (HS-CFRP-DL) configurations. The load-displacement curves for these specimens are illustrated in Fig. 11. The overall results of the flexural test are shown in Table 5.

The control HS displayed a peak load of 15.88 kN and failed at a displacement of 21.80 mm, with a brittle post-peak response.

The HS-CFRP-SL specimen achieved a peak load of 21.71 kN, indicating a 36.7% increase, and improved ductility with displacement reaching 30.15 mm.

The HS-CFRP-DL specimen exhibited the most enhanced behavior, attaining a peak load of 30.55 kN, a 92.4% increase over the control, and the highest displacement of 37.75 mm, demonstrating improved stiffness, ductility, and energy absorption.

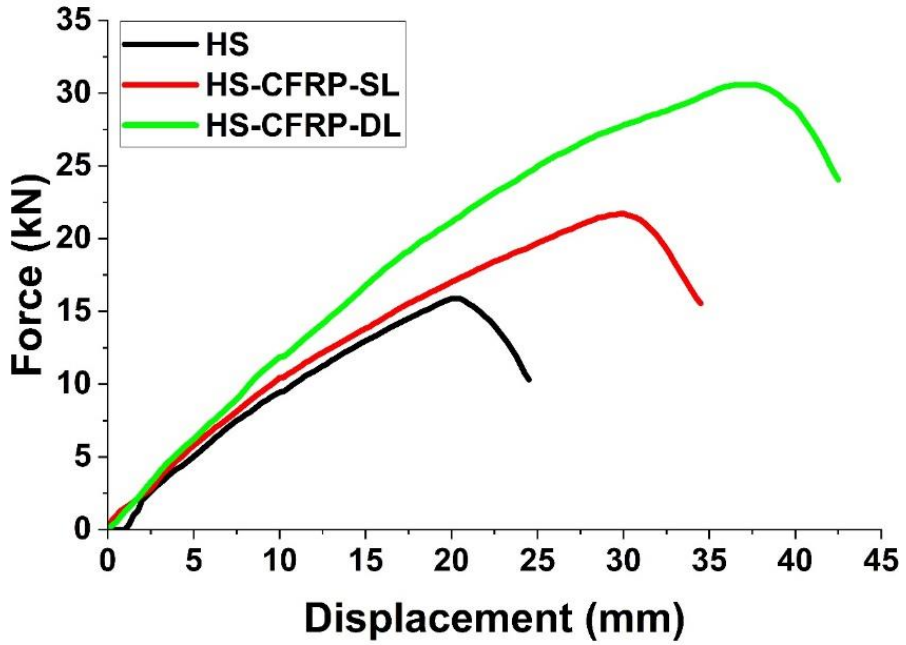

Fig. 11. Force-Displacement of Hollow Rectangular Sections.

Table 5. Flexural Performance of Rectangular Hollow Sections.

Specimen	Peak Load (kN)	Displacement at Peak (mm)	Load Improvement Over HS
HS (Control)	15.88	21.80	—
HS-CFRP-SL	21.71	30.15	+36.7%
HS-CFRP-DL	30.55	37.75	+92.4%

The flexural members failed primarily through two distinct mechanisms. In single-layer CFRP and GFRP configurations, debonding initiated at or near the beam ends, propagating toward mid-span under increasing flexural strain. In double-layer specimens, progressive delamination and rupture of the outer laminate layer occurred after yielding of the steel substrate. In hybrid-strengthened beams (with bolts), no sudden debonding was observed; instead, failure was governed by gradual fiber rupture and crushing at mid-span, accompanied by visible bolt hole deformation near the end anchor.

To strengthen the experimental findings, ductility and energy absorption were calculated for all flexural members using extracted values from the load-displacement plots, as shown in Fig. 10 and Fig. 11. Results show a significant enhancement in both ductility and energy absorption in CFRP-strengthened beams, with hybrid systems (HS-CFRP) offering the highest values. For instance, the HS-CFRP-DL beam achieved a ductility of 3 and absorbed 693 kN·mm of energy, compared to 2.2 and 176 kN·mm, respectively, for the control beam. This confirms the improved performance of the strengthening systems in resisting flexural failure.

Table 6. Ductility and Energy Absorption for each beam section.

Specimens	Ductility	Energy Absorption (kN.mm)
CS	2.22	140
CS-CFRP-SL	2.48	247
CS-CFRP-DL	3	363
HS	2.2	176
HS-CFRP-SL	2.83	442
HS-CFRP-DL	3	693

The double-layer CFRP effectively enhanced flexural stiffness, redistributed tensile stresses, and delayed crack propagation. Its superior displacement capacity underscores its potential in strengthening applications where high ductility and energy dissipation are essential.

5. Conclusions

This study comprehensively evaluated the structural performance of Carbon Fibre Reinforced Polymer (CFRP) and Glass Fibre Reinforced Polymer (GFRP) laminates for strengthening mild steel plates and beam sections under tensile and flexural loading. The experimental investigation included single- and double-layer laminates, surface-grooved substrates, and bolted anchorage systems, tested across different geometries, Channel Sections (CS) and Rectangular Hollow Sections (HS). Single-layer (SL) retrofits demonstrated limited effectiveness due to insufficient bond length, with GFRP-SL slightly underperforming compared to the unstrengthened specimen and CFRP-SL offering only marginal improvement. In contrast, double-layer (DL) configurations significantly enhanced strength and ductility, with CFRP-DL achieving a 27.34% increase in tensile capacity over the control. Surface grooving of SL specimens proved beneficial in improving bond quality and load resistance, especially for GFRP. However, it reduced ductility in CFRP, making it more suitable for stiffness-driven applications. Bolted anchorage in SL and DL systems further enhanced structural capacity and debonding resistance, with bolted CFRP-DL specimens delivering the highest tensile strength and a favorable balance between strength and ductility. Flexural tests confirmed the effectiveness of CFRP in enhancing both stiffness and peak load capacity, particularly in HS sections, where stress distribution was more uniform and local deformations were minimized.

In practical terms, CFRP offers superior performance but demands higher precision and cost, while GFRP provides economical and corrosion-resistant alternatives for moderate-strength applications. Grooving enhances bond efficiency but may reduce the net cross-section, and bolting adds mechanical reliability at

the expense of increased complexity. The selection of strengthening techniques should thus consider trade-offs among stiffness, ductility, installation feasibility, and structural geometry. Although both tensile and flexural behaviors were addressed, their retrofit responses revealed apparent differences, driven by load paths, cross-sectional geometry, and failure mechanisms, emphasizing the need for load-specific and geometry-sensitive retrofit strategies.

Looking forward, several avenues remain open for research. Future studies should investigate hybrid FRP systems that combine the advantages of CFRP and GFRP for cost-performance optimization. The structural behavior under fatigue loading or seismic cyclic actions also warrants detailed examination to assess long-term resilience. Overall, these future directions would contribute to developing robust, efficient, and durable FRP-based retrofitting strategies for steel infrastructure across diverse loading and environmental conditions.

Funding

This research did not receive any specific grant from funding agencies in the public, commercial, or not-for-profit sectors.

Conflicts of interest

The authors declare that they have no known competing financial interests or personal relationships that could have appeared to influence the work reported in this paper.

Authors contribution statement

Darshan Parakhiya: Data curation, Investigation, Methodology.

Husain Rangwala: Conceptualization, Writing – original draft, Writing – review & editing.

Amit Thoriya: Formal analysis, Writing – review & editing.

Tarak Vora: Resources, Supervision, Visualization, Validation.

References

[1] Harries Kent A, Dawood Mina. Behavior and Performance of Fiber-Reinforced Polymer-to-Steel Bond. Transp Res Rec 2012;2313:181–8. https://doi.org/10.3141/2313-19.

[2] Jiang X. Mechanical behaviour and durability of FRP-to-steel adhesively-bonded joints. 2013.

[3] Calabrese AS, Colombi P, D'Antino T. Analytical solution of the full-range behavior of adhesively bonded FRP-steel joints made with toughened adhesives. Eng Fract Mech 2023;292:109569. https://doi.org/10.1016/J.ENGFRACMECH.2023.109569.

[4] Zhang X, Wu Z, Cheng Y. An approach of steel plate hybrid bonding technique to externally bonded fibre-reinforced polymer strengthening system. Int J Distrib Sens Networks 2018;14. https://doi.org/10.1177/1550147718786455.

[5] Wang Z, Li C, Sui L, Xian G. Effects of adhesive property and thickness on the bond performance between carbon fiber reinforced polymer laminate and steel. Thin-Walled Struct 2021;158:107176. https://doi.org/10.1016/J.TWS.2020.107176.

[6] Ke L, Li Y, Li C, Cheng Z, Ma K, Zeng J. Bond behavior of CFRP-strengthened steel structures and its environmental influence factors: A critical review. Sustain Struct 2024;4:38.

[7] Hai-Tao W, Gang W, Yun-Tong D, Xiao-Yuan H. Experimental Study on Bond Behavior between CFRP Plates and Steel Substrates Using Digital Image Correlation. J Compos Constr 2016;20:4016054. https://doi.org/10.1061/(ASCE)CC.1943-5614.0000701.

[8] Liu Y, Chen W, Liu C, Li N. Bond Performance of CFRP/Steel Double Strap Joint at Elevated Temperatures. Sustain 2022;14. https://doi.org/10.3390/su142315537.

[9] Yang JQ, Smith ST, Feng P. Effect of FRP-to-steel bonded joint configuration on interfacial stresses: Finite element investigation. Thin-Walled Struct 2013;62:215–28. https://doi.org/10.1016/J.TWS.2012.07.020.

[10] Silva MAG, Biscaia H, Ribeiro P. On factors affecting CFRP-steel bonded joints. Constr Build Mater 2019;226:360–75. https://doi.org/10.1016/J.CONBUILDMAT.2019.06.220.

[11]Zhu F, Ke L, Feng Z, Zhou J, Li C, Zhang R. Enhancing bond performance of CFRP-steel epoxy-bonded interface by electrospun nanofiber veils. Thin-Walled Struct 2024;198:111765. https://doi.org/10.1016/J.TWS.2024.111765.

[12] El-Hamd OA, Sweedan A, El-Sawy K. Structural behavior of HFRP-steel double-lap joints with FRP bolts. World Congr Civil, Struct Environ Eng 2017:1–9. https://doi.org/10.11159/icsenm17.103.

[13] Marszałek J, Stadnicki J. Experimental and Numerical Study on Mechanical Behavior of Steel/GFRP/CFRP Hybrid Structure under Bending Loading with Adhesive Bond Strength Assessment. Materials (Basel) 2023;16. https://doi.org/10.3390/ma16145069.

[14] Sivasankar S, Sankar LP, Kumar AP, Shunmugasundaram M. Strengthening of square hollow steel sections using carbon fibre reinforced polymer strips subjected by compression. Mater Today Proc 2020;27:877–82. https://doi.org/10.1016/J.MATPR.2020.01.123.

[15] Rangwala H, Chandravadani S, Balagopal R. Damage Assessment and Strengthening of Transmission Line Tower at Component Level. J Struct Eng Manag 2016;3:9–15. https://doi.org/10.37591/josem.v3i3.4096.

[16] Rangwala H, Vora T. Application of Smart Computing in Steel Structural Health Monitoring: Sensor Based Damage Detection for Smart Infrastructures. Commun Comput Inf Sci 2025;2428 CCIS:195–211. https://doi.org/10.1007/978-3-031-86302-8_13.

[17] Jagtap PR, Pore SM. Effectiveness of CFRP composites on compression flange of structural I-beam. J Eng Des Technol 2019;17:782–92. https://doi.org/10.1108/JEDT-09-2018-0155.

[18] Weerasinghe KAB, Gamage JCPH, Fawzia S, Thambiratnam DP. Experimental investigation on flexural behaviour of vertically-curved circular-hollow steel sections strengthened with externally bonded carbon fibre reinforced polymer. Eng Struct 2021;236:112040. https://doi.org/10.1016/J.ENGSTRUCT.2021.112040.

[19] Regmi BB, Azadeh P. Fiber-Reinforced Polymer Strengthening of Steel Beams under Static and Fatigue Loadings. Pract Period Struct Des Constr 2021;26:4020046. https://doi.org/10.1061/(ASCE)SC.1943-5576.0000534.

[20] Li H, Xu S, Zhang Z, Song C. Experimental and numerical investigation on the corrosion effects on the bonding behavior between CFRP and steel. Compos Struct 2021;259:113465. https://doi.org/10.1016/J.COMPSTRUCT.2020.113465.

[21] Li C, Ke L, He J, Chen Z, Jiao Y. Effects of mechanical properties of adhesive and CFRP on the bond behavior in CFRP-strengthened steel structures. Compos Struct 2019;211:163–74. https://doi.org/10.1016/J.COMPSTRUCT.2018.12.020.

[22] Tafsirojjaman T, Fawzia S, Thambiratnam DP, Zhao XL. FRP strengthened SHS beam-column connection under monotonic and large-deformation cyclic loading. Thin-Walled Struct 2021;161:107518. https://doi.org/10.1016/J.TWS.2021.107518.

[23] Tafsirojjaman T, Fawzia S, Thambiratnam DP. Structural behaviour of CFRP strengthened beam-column connections under monotonic and cyclic loading. Structures 2021;33:2689–99. https://doi.org/10.1016/J.ISTRUC.2021.06.028.

[24] Hu L, Wang Y, Feng P, Wang HT, Qiang H. Debonding development in cracked steel plates strengthened by CFRP laminates under fatigue loading: Experimental and boundary element method analysis. Thin-Walled Struct 2021;166:108038. https://doi.org/10.1016/J.TWS.2021.108038.

[25] Liu ZQ, Luo B, Wang Q, Feng B. Experimental and numerical investigation of the anti-debonding performance for novel CFRP-steel tube composite member under tension. J Build Eng 2021;35:102004. https://doi.org/10.1016/J.JOBE.2020.102004.

[26] Tahmasebinia F, Zhang L, Park S, Sepasgozar S. Numerically Evaluation of FRP-Strengthened Members under Dynamic Impact Loading. Buildings 2021;11. https://doi.org/10.3390/buildings11010014.

[27] Kalfat R, Al-Mahaidi R. Mitigation of premature failure of FRP bonded to concrete using mechanical substrate strengthening and FRP spike anchors. Compos Part B Eng 2016;94:209–17. https://doi.org/10.1016/J.COMPOSITESB.2016.03.062.

[28] Alam MI, Fawzia S. Numerical studies on CFRP strengthened steel columns under transverse impact. Compos Struct 2015;120:428–41. https://doi.org/10.1016/J.COMPSTRUCT.2014.10.022.

[29] Janfada E, Nasseri H, Jahangir H. Performance Evaluation of Compressive Strength Models for SRP and SRG-Confined Concrete Columns. J Rehabil Civ Eng 2024;12. https://doi.org/10.22075/jrce.2023.30715.1855.

[30] Liu P, Xu C, Zhang Y, Chen L, Han Y, Liu R, et al. Detection and quantification of corrosion defects in CFRP-strengthened steel structures based on low-power vibrothermography. Nondestruct Test Eval 2025;40:585–609. https://doi.org/10.1080/10589759.2024.2326603.

[31] Soleymani A, Rezazadeh Eidgahee D, Jahangir H. Textile-reinforced mortar-masonry bond strength calibration using machine learning methods. Artif. Intell. Appl. Sustain. Constr., Elsevier; 2024, p. 301–15. https://doi.org/10.1016/B978-0-443-13191-2.00001-8.

[32] Wang S, Ge X, Su J, Fu Y. Experimental and numerical investigation of creep behaviour in adhesively bonded CFRP-steel joints. Constr Build Mater 2025;464:140234. https://doi.org/https://doi.org/10.1016/j.conbuildmat.2025.140234.

[33] Wang S, Fu Y, Su J, Duan Z, Yang S. Creep behaviour and modelling of adhesively bonded CFRP-steel joints. Thin-Walled Struct 2025;210:112981. https://doi.org/https://doi.org/10.1016/j.tws.2025.112981.

[34] Naseri Nasab M, Jahangir H, Hasani H, Majidi M-H, Khorashadizadeh S. Estimating the punching shear capacities of concrete slabs reinforced by steel and FRP rebars with ANN-Based GUI toolbox. Structures 2023;50:1204–21. https://doi.org/https://doi.org/10.1016/j.istruc.2023.02.072.

[35] Eidgahee DR, Soleymani A, Hasani H, Kontoni D-PN, Jahangir H. Flexural capacity estimation of FRP reinforced T-shaped concrete beams via soft computing techniques. Comput Concr 2023;32:1–13.

[36] Salih R, Zhou F, Abbas N, Mastoi AK. Experimental investigation of reinforced concrete beam with openings strengthened using frp sheets under cyclic load. Materials (Basel) 2020;13. https://doi.org/10.3390/ma13143127.

[37] Hamilton C, Bacon D, Mullis C, Mccarroll J, Davis M, Holt M, et al. Oregon Department of Transportation 2020:2020.

[38] Bocciarelli M, Colombi P. Elasto-plastic debonding strength of tensile steel/CFRP joints. Eng Fract Mech 2012;85:59–72. https://doi.org/https://doi.org/10.1016/j.engfracmech.2012.02.008.

[39] Hart-Smith LJ. Adhesive-bonded single-lap joints. 1973.